# Long-Term Stability of Planets in Binary Systems

Matthew J. Holman

Harvard-Smithsonian Center for Astrophysics, 60 Garden Street, Cambridge MA 02138 USA

and

Paul A. Wiegert

Dept. of Physics and Astronomy, York University, Toronto Ontario M3J 3P1 CANADA

# ABSTRACT

A simple question of celestial mechanics is investigated: in what regions of phase space near a binary system can planets persist for long times? The planets are taken to be test particles moving in the field of an eccentric binary system. A range of values of the binary eccentricity and mass ratio is studied, and both the case of planets orbiting close to one of the stars, and that of planets outside the binary orbiting the system's center of mass, are examined. From the results, empirical expressions are developed for both i) the largest orbit around each of the stars, and ii) the smallest orbit around the binary system as a whole, in which test particles survive the length of the integration ( $10^4$  binary periods). The empirical expressions developed, which are roughly linear in both the mass ratio  $\mu$  and the binary eccentricity e, are determined for the range  $0.0 \le e \le 0.7$ -0.8 and  $0.1 \le \mu \le 0.9$  in both regions, and can be used to guide searches for planets in binary systems. After considering the case of a single low-mass planet in binary systems, the stability of a mutually-interacting system of planets orbiting one star of a binary system is examined, though in less detail.

Subject headings: binaries: general — celestial mechanics — planetary systems

#### 1. Introduction

The long-standing question of whether planets can form and then persist in binary star systems appears to have been answered observationally. Planets have been detected about 55  $\rho^1$  Cancri,  $\tau$  Bootis and 16 Cygni B, all of which have companion stars (Butler et al. 1997; Cochran et al. 1997). Given that this basic question has been answered, one might now wonder what types of binary systems can harbor planets.

Rather than addressing the more difficult issue of how planets are formed in binary systems, a simple question of celestial mechanics is asked: in what regions of phase space near a binary system could low-mass planets persist for long times?

An extensive body of literature is dedicated to this question; just a few recent papers are noted here. The papers by Szebehely (1980) and Szebehely and McKenzie (1981) are examples of analytic work done on this problem. Graziani and Black (1981), Black (1982), and Pendleton and Black (1983) used numerical experiments of three body systems to develop empirical stability criteria. Hénon and Guyot (1970) numerically studied the stability of periodic orbits in the circular restricted problem as a function of the mass ratio. Although these studies were for generic systems, they were restricted to the case of the stars following circular orbits. Benest (1988; 1989; 1993; 1996) explicitly included the eccentricity of the binary in his studies of stability in the  $\alpha$  Centauri, Sirius and  $\eta$  Coronae Borealis systems. Dvorak (1984; 1986), Rabl and Dvorak (1988), and Dvorak et al. (1989) have studied the stability of test particles in binary systems with equal mass stars as a function of the binary eccentricity.

This body of literature has three principal limitations. First, although binaries typically have eccentric orbits, most of the analytic results have been developed for the case of binaries with circular orbits. Second, numerical investigations of stability have been restricted to special cases such as binary systems with equal mass stars or particular binary systems. Third, the numerical investigations been limited to fairly short integrations. However, the rapid increase in processor speed and improved algorithms make it a straightforward task to extend the numerical results.

Orbits in binary systems have been traditionally separated into three categories. Following the designations of Dvorak and Rabl (1986), the first includes planetary or P-type orbits. These are well outside the binary, where the planet essentially orbits the center of mass of the stars. The second type refers to the satellite or S-type orbits. These are orbits near one of the stars, with the second star considered to be a perturber. The third type refers to orbits near the  $L_4$  or  $L_5$  triangular Lagrange points. These orbits are not normally of interest for binary systems as the mass ratio must be less than  $\mu = m_2/(m_1 + m_2) \approx 0.04$  for motion about these points to be linearly stable.

In this study, both P and S-type orbits are examined. However, the results for the S-type orbits, those close to one of the stars, are more directly applicable to current extrasolar planet searches, as radial velocity variations are more easily detected in systems in which the planets are

close to one of the stars. It is our hope that the results of our investigation can be used as a guide in selecting a sample of suitable candidates for a radial velocity survey of binary systems.

This work is different from that which precedes it in two ways: (1) a full range of mass ratios has been examined, as well as a full range of eccentricities; (2) these integrations extend for much longer times than have been examined in the past.

In addition to looking at the stability of single planets in binary systems, the stability of systems of multiple planets in eccentric binaries is also investigated, albeit briefly. Interactions between planets may affect their stability through angular momentum transfer or other mechanisms. The results of this part of the investigation help us to understand the limits of results obtained for single planets.

#### 2. Method

This study investigates orbital stability numerically within the elliptic restricted three body problem. That is, the planets are modeled as test particles moving in the gravitational field of a pair of stars on fixed eccentric orbits about each other. As the test particles do not interact with each other, this approach allows us to simulate large numbers of single planet systems simultaneously.

An approach first used by Dvorak (1986) is adopted here. First, an eccentricity, mass ratio, and initial orbital longitude for the stars is chosen. Second, a battery of test particles on orbits in or near the binary is started. These particles are on initially circular, prograde orbits in the plane of the binary. This choice is based on the results from the  $\alpha$  Centauri system (Wiegert and Holman 1997) in which the largest stable orbit near the stars was found to have an inclination in the plane of the binary<sup>1</sup>. For a range of semimajor axes, test particles are started at eight uniformly spaced orbital longitudes.

Given the initial conditions of the binary system and the test particles, the system is numerically integrated. During the course of the integration close encounters between the test particles and stars are checked for, close encounters defined arbitrarily to be a passage within 0.25 of the binary semimajor axis  $a_b$  of the non-central star. Escape orbits are also monitored. Any test particle that encounters one of the stars or escapes is removed from the integration. At the end of the integrations, the semimajor axis at which the test particles at all initial longitudes survived the full integration time is determined. We call this the critical semimajor axis  $^2$ . The critical semimajor axis determines the stability limit on the time scale of the numerical integration. Note

<sup>&</sup>lt;sup>1</sup>More precisely, the largest stable orbits were those that were retrograde in the binary plane, but these were only slightly (10%) larger than those at zero inclination.

<sup>&</sup>lt;sup>2</sup>Rabl and Dvorak (1988) refer to this as the Lower Critical Orbit.

Table 1: Initial conditions for the binaries and test particles. The binary semimajor axis is  $a_b$ , its eccentricity is e, its mass ratio  $\mu = m_2/(m_1 + m_2)$ . A test particle's initial semimajor axis, eccentricity, inclination relative to the binary plane, longitude of the ascending node, argument of perihelion and mean anomaly are designated by a,  $e_p$ , i,  $\Omega$ ,  $\omega$  and M respectively.

Inner region	Outer region										
Binaries											
$a_b = 1.0$											
$0.1 \le \mu \le 0.9$	$0.1 \le \mu \le 0.5$										
	$\Delta\mu = 0.1$										
$0.0 \le e \le 0.8$	$0.0 \le e \le 0.7$										
	$\Delta e = 0.1$										
Binary phas	se: periapse or apoapse										
Γ	Cest particles										
$0.02 \le a \le 0.5a$	$b   1.0 \le a \le 5.0a_b$										
$\Delta a = 0.0025 \text{-} 0.01$	$a_b \qquad \Delta a = 0.1 a_b$										
$e_p = i = \Omega = \omega = 0.0$											
$M = 0^{\circ}, 45^{\circ}, 90^{\circ},$	$135^{\circ}, 180^{\circ}, 225^{\circ}, 270^{\circ}, 315^{\circ}$										

that this approach assumes that the critical semimajor axis is well-defined (i.e. that the boundary between stable and unstable regions is sufficiently sharp); however, this will be shown to be a valid assumption in most cases.

Binaries with eccentricities in the range  $0.0 \le e \le 0.7$ -0.8 and mass ratio in the range  $0.1 \le \mu \le 0.9$  have been examined, though only the range  $0.1 \le \mu \le 0.5$  has been studied in the outer region, since systems with mass ratios of  $\mu$  and  $1 - \mu$  are equivalent in this regime (with the exception of a 180° change in the particles' longitudes). By the mass ratio  $\mu = m_2/(m_1 + m_2)$  is meant, where  $m_1$  is the mass of the star the test particle is orbiting and  $m_2$  is the mass of the perturbing star. For equal mass stars  $\mu = 0.5$ . Both the eccentricities and mass ratios have been explored in increments of 0.1 or less. The initial phase of the binary orbit is also a free parameter. The two extremes are examined: the binary initially at periapse and initially at apoapse, and the more conservative result is taken (*i.e.* that for which the stable region is smallest), though the results do not differ significantly on this account. The initial conditions of our primary suite of simulations are summarized in Table 1.

For the orbital integrations the symplectic mapping method of Wisdom and Holman (1991) was used. Although this technique was developed for numerically integrating systems of planets with a single dominant central mass, it can also be applied to binary systems for orbits close to one of the stars, when the other star is a distant perturber. For orbits in the intervening region, where the forces from the two stars are comparable, two techniques are used. First, the symplectic mapping method is employed, but with a smaller time step. Second, a conventional Bulirsch-Stoer integrator is used. The region for which the symplectic mapping method is not well-suited is also the region in which test particles quickly escape, thus it is not necessary to use an efficient method

Table 2: Planet survival times in the inner region, with  $\mu = 0.5$  and e = 0.5. Columns 1-8 show survival times for planets in positions 1-8 with the stars started at periapse. Column 9 shows the initial semimajor axis of the planets in units where the binary semimajor axis is unity. Columns 10-18 give the survival times with the stars started at apoapse. All times are given in units of 10 binary periods. A "+" indicates the test particle survived  $10^4$  binary periods. Here the critical semimajor axis is 0.12, the farthest semimajor axis at which all the planets survived the full integration. Several of the test particles on the stability boundary were terminated at times longer than the 300 binary periods integrated by Rabl and Dvorak (1988), but the stability boundary was not shifted significantly by extending the integration to  $10^4$  binary periods.

	Binary initially at periapse									Binary initially at apoapse						
P1	P2	Р3	P4	P5	P6	Ρ7	P8	a	A1	A2	A3	A4	A5	A6	A7	A8
3	1	1	1	3	2	1	1	0.17	1	1	1	1	1	1	1	1
7	1	1	1	2	1	2	1	0.16	1	1	1	1	1	6	1	1
13	2	1	1	5	2	1	2	0.15	3	2	2	1	8	2	2	2
57	7	3	12	39	7	1	6	0.14	+	9	7	4	7	18	7	13
192	159	11	106	+	53	62	56	0.13	776	+	+	119	267	142	511	+
+	+	+	+	+	+	+	+	0.12	+	+	+	+	+	+	+	+
+	+	+	+	+	+	+	+	0.11	+	+	+	+	+	+	+	+
+	+	+	+	+	+	+	+	0.10	+	+	+	+	+	+	+	+
+	+	+	+	+	+	+	+	0.09	+	+	+	+	+	+	+	+
	+	+	+	+	+	+	+	0.08	+	+	+	+	+	+	+	+

in this region.

# 3. Single planet results: inner region

Table 2 shows an example of the results of the numerical integrations in the inner region. It lists the times survived by test particles as a function of initial orbital longitude and semimajor axis. This example is for  $\mu = 0.5$  (equal mass stars) and e = 0.5. The times are given in units of 10 binary periods. A "+" marks those test particles that survived the full  $10^4$  binary period integration. For this eccentricity and mass ratio the critical semimajor axis is  $a_c = 0.12$ , as all test particles at or interior to this value survived the full integration. Those with the longest removal times lie along the boundary, with removal time decreasing outward.

Rabl and Dvorak (1988) concluded that an integration time of 300 binary periods was adequate to determine the gross stability boundary. Here it is seen that several of the test particles on the stability boundary were terminated at times longer than the 300 binary periods, but the stability boundary was not shifted significantly by extending the integration to 10<sup>4</sup> binary periods. Ten thousand binary periods is still short compared to the ages of binary systems; therefore it is possible that longer-term instabilities will arise.

Table 3: The critical semimajor axis in units of the binary semimajor axis for each pair of values of the mass ratio and eccentricity in the inner region. These empirical results are from the  $10^4$  binary period numerical integrations.

		0								
	$\mu$	0.10	0.20	0.30	0.40	0.50	0.60	0.70	0.80	0.90
e										
0.0		0.45	0.38	0.37	0.30	0.26	0.23	0.20	0.16	0.13
0.1		0.37	0.32	0.30	0.27	0.24	0.20	0.18	0.15	0.11
0.2		0.34	0.27	0.25	0.23	0.20	0.18	0.16	0.13	0.10
0.3		0.28	0.24	0.21	0.19	0.18	0.16	0.14	0.12	0.09
0.4		0.23	0.20	0.18	0.16	0.15	0.13	0.11	0.10	0.07
0.5		0.18	0.16	0.14	0.13	0.12	0.10	0.09	0.08	0.06
0.6		0.13	0.12	0.11	0.10	0.09	0.08	0.07	0.06	0.045
0.7		0.09	0.08	0.07	0.07	0.06	0.05	0.05	0.045	0.035
0.8		0.05	0.05	0.04	0.04	0.04	0.035	0.03	0.025	0.0225

The most important number derived from Table 2 is the critical semimajor axis. For each pair of values of  $\mu$  and e this number is measured. These are listed in Table 3. From these numbers an empirical expression that gives the critical semimajor axis as a function of  $\mu$  and e can be derived. A least squares fit to the data yields:

$$a_c = [(0.464 \pm 0.006) + (-0.380 \pm 0.010)\mu + (-0.631 \pm 0.034)e + (0.586 \pm 0.061)\mu e + (0.150 \pm 0.041)e^2 + (-0.198 \pm 0.074)\mu e^2]a_b,$$
(1)

where  $a_c$  is the critical semimajor axis,  $a_b$  is the binary semimajor axis, e is the binary eccentricity, and  $\mu$  is the mass ratio. Each coefficient is listed along with its formal uncertainty; the expression is valid to within 4% (typically) and 11% (worst-case) over the range of  $0.1 \le \mu \le 0.9$  and  $0.0 \le e \le 0.8$ . The expression was chosen to provide a reasonable fit with a minimum of terms. It is arbitrary that the function is linear in  $\mu$  but quadratic in e.

# 3.1. Hill's regime

As  $(1 - \mu)$  and  $\mu \to 0$ , one would expect the critical semimajor axis to scale as with the Hill's sphere *i.e.* as  $O(\mu^{1/3})$  or  $O[(1 - \mu)^{1/3}]$ , an effect which is not predicted by Eq. 1. In order to investigate, the simulations at e = 0.0 were extended to a series of values in the range  $0.9 \le \mu < 1.0$ . A plot of  $a_c$  as a function of  $\mu$  is shown in on a log-log scale in Fig. 1. The approximate linearity of  $a_c$  in  $\mu$  changes to the expected  $(1 - \mu)^{1/3}$  dependence as the mass of the primary and secondary diverge. These results imply two distinct dynamical regimes for third-particle stability, one where  $(1 - \mu)$  and  $\mu \ll 1$  and one for  $\mu \sim 0.5$ , with the switch occurring near where  $(1 - \mu)$  and  $\mu \sim 0.2$ .

# 3.2. Comparison with earlier work

Rabl and Dvorak (1988) report the following expression for the critical semimajor axis in the case of equal mass stars:

$$a_c = [(0.262 \pm 0.006) + (-0.254 \pm 0.017)e + (-0.060 \pm 0.027)e^2]a_b$$

Inserting  $\mu = 0.5$  into Eq. 1 and collecting error terms one gets:

$$a_c = [(0.274 \pm 0.008) + (-0.338 \pm 0.045)e + (0.051 \pm 0.055)e^2]a_b$$
 (2)

In both cases it appears that a linear fit in e would also work. The two expressions are consistent, although our expression has a somewhat sharper dependence on e. Fig. 3 shows the data and least squares fit expression for the marginal case of  $\mu=0.5$ . The solid line is our least squares fit; the dashed line is that of Rabl and Dvorak (1988). They only explored up to e=0.6; their line deviates most from ours when it is extrapolated beyond e=0.6. As longer integrations might tend to bring the entire curve down, it is clear that this is not an important difference between the investigations. The fits are more strongly affected by the end points than by the integration length. Fig. 2 shows the data and empirical fit for the marginal case of e=0.5. It is notable that for this range of mass ratio the change in  $a_c$  is very linear. For much larger or smaller values of  $\mu$ , the  $O(\mu^{1/3})$  or  $O[(1-\mu)^{1/3}]$  scalings of the Hill's sphere occur (§ 3.1).

Aside from the work of Rabl and Dvorak (1988), there are other results to which ours can be compared. As noted above, Benest (1988, 1989, 1993, 1996) studied the  $\alpha$  Centauri, Sirius and  $\eta$  Coronae Borealis systems (looking only at orbits in the plane of the binary). We concentrate on his results for the  $\alpha$  Centauri system. The two stars in the tight binary of the  $\alpha$  Centauri system have masses  $\mu_A = 0.54$  and  $\mu_B = 0.46$  and e = 0.52. Although Benest uses a rotating-pulsating coordinate system that makes it difficult to interpret his results, for  $\alpha$  Cen B he finds stability limits of about  $a_c = 0.19a_b$  and  $a_c = 0.15a_b$  for the stars started at periapse and apoapse, respectively. For  $\alpha$  Cen A, Benest only gives the results for the stars started at periapse. He finds  $a_c = 0.23a_b$ . Our empirical expression yields  $a_c = 0.11a_b$  and  $a_c = 0.12a_b$ , for  $\alpha$  Cen B and A, respectively. It is unclear why Benest's results indicate a much larger (up to a factor of two) stable region than our own, when Rabl and Dvorak's, though only a factor of three longer than Benest's, are so much closer to our results. Perhaps the most unstable particles leave on time scales of between one and a few hundred binary periods, with the remainder evolving more slowly.

Wiegert and Holman (1996) recently studied the  $\alpha$  Centauri system in detail, and examined the dependence of stability on inclination. For prograde orbits in the plane they find a limit of  $a_c = 0.11a_b$ , but used a much longer integration time (3 × 10<sup>5</sup> binary periods). This suggests that the strongest instabilities acting on time scales less than  $\sim 10^6$  binary periods reveal themselves rather quickly (10<sup>2</sup>–10<sup>3</sup> periods); however, longer time scales instabilities remain a possibility.

Table 4: Critical semimajor axes for the binary systems listed in Dvorak et al. (1989). For each system the period (in years), parallax (in arcseconds), semimajor axis (in AU), and eccentricity are listed. Following the eccentricity we list the larger mass (in solar masses) and the critical semimajor axis (in AU) and period (in years) of a test particle orbiting about larger mass exactly at the critical semimajor axis. In the next six columns we list the mass, critical semimajor axis, and critical period for the smaller mass in the binary, and then the total mass along with  $a_c$  and the period for the outer (P-type) region.

Name	Period	Prlx.	a	e	$m_1$	$a_{c1}$	$p_1$	$m_2$	$a_{c2}$	$p_2$	M	$a_{cP}$	$p_P$
ADS 520	25.0	0.07	9.57	0.22	0.7	1.93	3.21	0.7	1.93	3.21	1.40	29	129
$\epsilon$ Cet	2.67	0.069	1.57	0.27	1.3	0.29	0.14	1.3	0.29	0.14	2.60	4.9	6.7
$\gamma$ Vir	171.37	0.090	37.84	0.881	0.94	0.61	0.49	0.90	0.60	0.49	1.84	158	1467
$\alpha$ Com	25.87	0.038	12.49	0.5	1.43	1.49	1.52	1.37	1.45	1.49	2.80	45	182
$\epsilon \text{ CrB}$	41.56	0.059	13.98	0.276	0.79	2.59	4.68	0.78	2.57	4.66	1.57	44	231
ADS 9716	55.88	0.048	19.15	0.591	1.135	1.76	2.20	1.135	1.76	2.20	2.27	72	407
BD $-8^{\circ} 4352$	1.72	0.152	1.35	0.05	0.42	0.35	0.32	0.42	0.35	0.32	0.84	3.4	6.9
BD $45^{\circ} 2505$	12.98	0.160	4.58	0.73	0.285	0.25	0.23	0.285	0.25	0.23	0.57	18	103
ADS 11871	61.2	0.061	22.96	0.249	1.647	4.49	7.40	1.582	4.37	7.26	3.23	71	330
$\delta$ Equ	5.7	0.052	4.73	0.42	1.658	0.67	0.43	1.593	0.66	0.42	3.25	16	36.8
Kpr 37	21.85	0.074	9.67	0.15	1.2	2.38	3.35	0.89	1.96	2.90	2.09	28	102
99 Her	55.8	0.060	16.39	0.74	0.888	0.97	1.01	0.522	0.73	0.87	1.41	68	475
9 Pup	23.26	0.067	10.00	0.69	0.98	0.67	0.56	0.87	0.63	0.54	1.85	40	184
$ADS\ 15972$	44.60	0.248	9.53	0.41	0.2728	1.57	3.76	0.167	1.17	3.11	0.44	34	302
$\alpha$ CMa	50.09	0.375	19.89	0.592	2.11	2.17	2.20	1.04	1.48	1.76	3.15	79	398
$\alpha$ Cen	79.92	0.760	23.57	0.516	1.12	2.79	4.40	0.95	2.54	4.15	2.07	87	567
$\xi$ Boo	151.51	0.147	33.14	0.512	0.858	3.96	8.51	0.731	3.61	8.02	1.59	123	1076

#### 3.3. Comparison with real binary systems

In Table 4 the binary systems listed in Dvorak et al. (1989) are re-examined. For each system the period (years), parallax (arcseconds), semimajor axis (AU), eccentricity, mass of the primary (solar masses), the critical semimajor axis for test particles orbiting about the larger mass, and the period (in years) of a test particle at the critical semimajor axis. Following that the mass of the secondary star, its critical semimajor axis, and critical period are listed, and then the values for the outer region (§ 4). Our empirical expression (Eq. 1) has been used to determine the critical semimajor axes for these systems. The periods of the critical orbits follow simply from the mass of the central star and the critical semimajor axis.

Although we make no statement about the process of forming planets in binary systems, we note that the periods of small bodies orbiting at the critical semimajor axis in these systems is longer than the orbital periods of most of the recently discovered extra-solar planets.

Table 5: Basic data for the three binary systems thought to contain planets, along with a comparison with the critical semimajor axes of the systems with those of the planets (Hoffleit and Jaschek 1982; Butler et al. 1997; Cochran et al. 1997). The binary's semimajor axis is assumed to be equal to the projected radius. Some values are estimates. Note that two planets have been detected in the  $55 \rho^1$  Cnc system.

	16 Cyg B	$55 \rho^1 \text{ Cnc}$	$\tau$ Boo
HR number	7504	3522	5185
MK type	G2.5V	G8V	F6IV
companion MK type	G1.5V	M2	M2
binary $\mu$	$\sim 0.5$	$\sim 0.8$	$\sim 0.9$
binary $r$ (AU, projected)	1000	1200	100
binary $e$	???	???	???
planet $M \sin i \ (M_J)$	1.5	0.84, > 5	3.87
planet $a$ (AU)	1.72	0.11, > 4	0.0462
planet $\tau$ (days)	800	$14, \sim 2800$	3.3
planet $e$	0.63	0.05, ???	0.02
$a_c$ (AU) if binary $e = 0.0$	260	200	13
$a_c$ (AU) if binary $e = 0.8$	40	30	2.3

Returning to the recently discovered planets in binary systems, our results can be compared with the sizes of the planetary orbits found. The data summarised in Table 5. The size of the binary orbits and eccentricities of these binaries are not known. Their projected separation has been taken as the semimajor axis and the critical semimajor axis has been computed for the extremes e = 0 and e = 0.8. The orbits of the planets are within the critical semimajor axis in all cases, however, the radial velocity measurements used to find these planets are strongly biased towards planets very close to their companion stars.

As stated, the results here concern the gross orbital stability of planets orbiting in the plane of the binary system. Roughly speaking, we have identified the regions of phase space in which the perturbations in the with perturbations of the binary are strong enough to significantly alter the semimajor axis of the planet. However, the weak perturbations of a distant binary companion can lead to large amplitude eccentricity oscillations for orbits that are inclined more than about 40 degrees with respect to the binary plane. Even when the orbital period of the binary is long enough compared to that of the planet that the planets semimajor axis is adiabatically preserved, the eccentricity oscillation can be large enough to drive the planet at periapse into the surface of the central star (Holman et al. 1997; Wiegert and Holman 1997).

Table 6: Planet survival times in the outer region, with  $\mu = 0.3$ , e = 0.4. Columns 1-8 show survival times for planets in positions 1-8 with the stars started at periapse. Column 9 shows the initial semimajor axis of the planets in units where the binary semimajor axis is unity. Columns 10-18 give the survival times with the stars started at apoapse. All times are given in units of 1000 binary periods. A "+" indicates the test particle survived  $10^4$  binary periods.

	Binary initially at periapse										Binary	initial	lly at a	poapse		
P1	P2	P3	P4	P5	P6	P7	P8	a	A1	A2	A3	A4	A5	A6	A7	A8
0.25	0.25	0.43	0.81	0.21	1.1	0.75	0.75	3.1	0.81	0.24	4.4	2.7	0.48	0.4	2.3	6.5
0.31	1.31	1.31	0.76	0.43	1.6	1.6	1.3	3.2	5.3	0.44	0.80	0.49	2.5	1.1	0.70	0.86
0.37	0.4	0.4	1.0	0.91	0.53	3.8	0.56	3.3	2.7	0.56	0.53	0.53	0.64	0.54	0.89	0.73
2.5	0.76	0.67	1.3	1.2	0.76	0.65	0.1.1	3.4	+	1.3	2.1	1.6	+	5.9	9.2	0.67
0.48	0.3	0.62	1.1	2.0	0.17	0.33	0.48	3.5	+	+	+	+	+	+	+	+
+	+	+	+	+	+	+	+	3.6	+	+	+	+	+	+	+	+
2.9	1.8	1.8	2.3	0.45	1.2	1.1	6.2	3.7	+	4.1	+	6.4	+	+	+	1.35
+	+	+	+	+	+	+	+	3.8	+	+	+	+	+	+	+	+
+	+	+	+	+	+	+	+	3.9	+	+	+	+	+	+	+	+
+	+	+	+	+	+	+	+	4.0	+	+	+	+	+	+	+	+

### 4. Single planet results: outer region

The results in the outer region are similar in some respects to those in the inner region: the transition from the unstable region near the binary to the stable region further outside occurs over a small range in semimajor axis. For this reason, a simple empirical expression for the stability boundary can be devised, as was done for the inner region. However, an additional complication arises. In a large fraction of the cases simulated, an additional island of instability is seen beyond the inner "boundary" of the stable region. This result is most easily seen by an example. Table 6 shows the results of a outer region simulation, in the format of Table 2 for  $\mu = 0.3$  and e = 0.4. A island of instability exists outside the inner unstable region: in this case, the island arises near  $a = 3.7a_b$ . Such islands are seen in most of the simulations. They do not always occur at  $a = 3.7a_b$ ; rather, they occur at the innermost n : 1 mean motion resonance outside the inner unstable region. Such instability islands are seen at the 3:1 through the 9:1 mean-motion resonances under various circumstances (the resonance revealed in Table 6 is the 7:1), and have been seen in previous studies (e.g. Hénon and Guyot 1970; Dvorak 1984; Hagel and Dvorak 1988, Dvorak et al. 1989).

The phenomenon described above clearly implies that there is not a sharp boundary between stable and unstable regions. It seem quite possible that, if our simulations were extended, instability would arise further and further from the central pair at higher and higher order mean motion resonances. However, whether such resonances would overlap sufficiently to render a large fraction of this outer "stable" region unstable is unclear.

Since the processors and numerical integration techniques at our disposal do not allow us to resolve this situation through continued simulations, we simply present the results obtained so

Table 7: The critical semimajor axis in units of the binary semimajor axis for each pair of values of the mass ratio and eccentricity in the outer region. These empirical results are from the  $10^4$  binary period numerical integrations.

	$\mu$	0.10	0.20	0.30	0.40	0.50
e						
0.0		2.0	2.2	2.3	2.3	2.3
0.1		2.4	2.7	2.7	2.8	2.8
0.2		2.7	3.1	3.1	3.1	3.1
0.3		3.1	3.5	3.5	3.3	3.2
0.4		3.5	3.5	3.6	3.5	3.6
0.5		3.8	3.9	3.9	3.6	3.7
0.6		3.9	3.9	3.9	3.8	3.7
0.7		4.2	4.3	4.3	4.1	4.1

far here, with the caveat that further investigation is likely to prove them incomplete. Since the region in which planets *could* survive is of most interest here, the innermost semimajor axis at which planets at all eight longitudes survive is chosen as our critical semimajor axis. With this choice comes the clear possibility that some planets with semimajor axes in excess of this value will be unstable. However, since our goal is to provide a guide to observational searches and the planets closest to the central stars will likely prove the easiest to detect (by direct imaging surveys, say), one wishes to avoid placing overly pessimistic limits on the stability region at this time. The critical semimajor axes are listed in Table 7.

The critical semimajor axis is only a weak function of  $\mu$ , though again roughly linear in e over the range explored here. There is a weak dependence on  $\mu$  however, evidenced by a low broad peak at  $\mu \sim 0.25$ . This peak is also seen in analyses of the Hill's stability of the restricted three-body problem (Szebehely 1980; Szebehely and McKenzie 1981). Because of this feature, up to second order terms in  $\mu$  are allowed in the fit in this case.

Our expression for the fit is

$$a_c = (1.60 \pm 0.04) + (5.10 \pm 0.05)e + (-2.22 \pm 0.11)e^2 + (4.12 \pm 0.09)\mu + (-4.27 \pm 0.17)e\mu + (-5.09 \pm 0.11)\mu^2 + (4.61 \pm 0.36)e^2\mu^2$$
(3)

The terms in  $e^2\mu$  and  $e\mu^2$  have been omitted because their addition provided little improvement of the fit. The residuals of Eq. 4 show it to be good to 3% typically, and to 6% worst-case over the range  $0.0 \le e \le 0.7$  and  $0.1 \le \mu \le 0.9$  in the outer region. Table 4 lists the values of the outer critical orbit for the real binary systems examined by Dvorak et al. (1989).

#### 4.1. Comparison with earlier work

Our results are very similar to those obtained by Dvorak et al. (1989) even though our simulations are 20 times longer. They find the critical semimajor axis to be essentially independent of  $\mu$ , and provide an expression for it in their Eq. (2). However, a comparison of their expressions with their data leads us to suspect that their Eqs. (1) and (2) may have their labels switched. Their Eq. (1) matches their data for their "upper critical orbit" (our "critical semimajor axis") much better than Eq. (2). If the equations are mislabelled, their empirical expression is

$$a_c = 2.37 + 2.76e - 1.04e^2. (4)$$

Performing a least-squares fit in the eccentricity, our data points produce

$$a_c = (2.278 \pm 0.008) + (3.824 \pm 0.33)e - (1.71 \pm 0.10)e^2.$$
 (5)

with residuals indicating that this expression is within 5% of the experimental value typically, 14% worst case. Dvorak et al. do not provide information on their residuals, but compare their empirical expression with numerical results for a few independent (i.e. real) binary systems. They show slightly smaller errors (typical: within 2%; worst case: within 10%), but their error analysis is limited to only seven independent cases, and only examined what they call the Lower Critical Orbit (i.e. the largest semimajor axis at which all test particles become unstable). A comparison of our and their data points with the empirical expressions is provided by Fig. 4. We note that our data contains five points for each value of e, corresponding to  $\mu \in \{0.1, 0.2, 0.3, 0.4, 0.5\}$ .

Our data points follow the same general trend as those of Dvorak et al. but typically at slightly larger values. This result indicates that, though the edge between stable and unstable regions may not evolve quickly, the stable region does erode as the time scales considered lengthen, at least at higher binary eccentricities.

We also note that our results are comparable to Szebehely and McKenzie's (1981) analytical results. They computed the Hill's stability criterion for the circular restricted three-body case, and found critical radii  $r \approx 2.24$ , 2.4, and 2.17 $a_b$  for  $\mu = 0.1$ , 0.24, and 0.5. Our numerical results for e = 0.0 provide  $a_c \approx 2.0$ , 2.25, and 2.3 $a_b$  for the same values of  $\mu$ . The closeness of these results confirms the validity of these numerical integrations, and hints that the Hill's stability criterion may provide more insight into the question of the stability of planets in binary star systems.

Lastly, Wiegert and Holman (1997) found that the outer critical semimajor axis  $a_c = 3.7a_b$  for central binary of  $\alpha$  Cen ( $e = 0.52, \mu = 0.45$ ). This value is very close to the values derived here,  $3.73a_b$  from Eq. 4 and  $3.8a_b$  from Eq. 5, though their integrations ran over three times longer (32000 binary periods) than those presented here.

# 5. Multiple planet results

Now that stability limits have been derived for test particles orbiting near one of the stars in a binary system, we consider systems with multiple planets. Innanen et al. (1997) examined the specific effects of a binary companion on the orbits of the planets in our Solar System. We ask a similar but slightly different question: if our own Solar System had a solar mass companion in an eccentric orbit how large would its semimajor axis need to be for the planets to survive  $O(10^9 \text{ yr})$ ?

This question is addressed with numerical experiments. In the first set of experiments the system of our own Sun and the four giant planets, Jupiter through Neptune, is augmented with a solar mass companion and then numerical integrated for times up to one billion years. The companion was initially placed in the invariable plane of the solar system with  $\Omega = \omega = M = 0^{\circ}$ . The eccentricity of the companion was 0.4. Several initial semimajor axes of the companion were tested, and for each value of the initial semimajor axis the system was integrated until the planetary orbits began to cross or became hyperbolic with respect to the Sun. Semimajor axes from 150 AU to 500 AU in increments of 50 AU. For all companion semimajor axes except 400 and 500 AU Uranus and Neptune cross orbits within  $10^7-10^8$  years. In the 400 and 500 AU the systems survive the full  $10^9$  year integrations. That the 400 AU system survived but the 450 AU system did not may indicate that particular configurations may have additional stability arising from factors other than the distance of the perturber.

In the second set of experiments we test the effect of a highly inclined solar mass companion on a system of multiple planets. Again we start with our own Sun and giant planets. To this we add a solar mass companion inclined at 87° and 75° to the invariable plane of the Sun and planets. The companion is started with  $\Omega = \omega = M = 0^{\circ}$  and e = 0.4, and a = 500, 750, and 1000 AU. The 500 and 750 AU runs are unstable in  $10^7-10^8$  years, but the 1000 AU runs survive  $10^9$  years. In these runs the planets maintain their semimajor axes, eccentricities, and relative inclinations, but the plane of the planets regresses about the normal to the binary orbit. The  $i = 75^{\circ}$  run has a 110 Myr regression period; the  $i = 87^{\circ}$  run has a 400 Myr regression period.

We can compare the results of these experiments to those predicted by Eq. 1. For  $a_b = 400$  AU,  $\mu = 0.5$ , and e = 0.4 we predict  $a_c = 59$  AU. Neptune's semimajor axis is  $a_N = 30$  AU. Our empirical expression overestimates the critical semimajor axis by a factor of 2. This is partly because, with a system of interacting planets, it is not necessary to completely strip one of the planets from its star to disrupt the system. It is only necessary to perturb the planetary eccentricities enough that the planets strongly interact. Nevertheless, even with this factor of 2, it is reassuring that the simple results from the elliptic restricted three body problem predict the correct scale of the stability limit in our Solar System.

#### 6. Summary and Future Work

We have numerically investigated the long-term stability of planets near one of the stars in a binary system. Unlike earlier studies, we have examined a full range of mass ratios and eccentricities. From the results we have derived an empirical expression for the semimajor axis inside of which test particles on initially circular orbits survive the full integration. This expression is given as a function mass ratio and semimajor axis. Our results for the inner S-type region are confirmed, albeit weakly, by observations of planets in extrasolar binary systems. Where our results examine parameter values studied by earlier investigators, our results are largely consistent, despite our significantly longer integration times. This fact indicates that the stable/unstable boundary remains consistent over a wide range of time scales, though some evidence for the erosion of the stable regions over time has been seen. A further important proof of concept is that systems of multiple planets, as modeled by our own outer planets, can remain stable for times of order a billion years in the inner S-type region of an eccentric binary system.

There are several avenues of future work in this field:

- Here we have developed a very crude understanding of the limits of stability. Particular isolated regions of phase space near a binary system, at the location of particular resonances, will have different stability properties. The instabilities associated with the n:1 mean-motion resonances (§ 4), of which only a cursory examination has been made here, are clear evidence of this.
- Despite the coincidence of our numerically computed stability boundary with that derived analytically for Hill's stability by Szebehely and McKenzie (1981), as yet we have no analytic derivation of the stability limit, nor do we have a precise understanding of the source of the chaos observed near and beyond the limit. A semi-analytic stability criterion based on the boundary between chaotic and quasiperiodic motion is presented in Mardling and Aarseth (1998).
- The effects of giving the planets initial non-zero eccentricities, has as yet been studied in only a very few cases (Benest 1988; 1989; 1996).

#### 7. Acknowledgements

We thank S. Tremaine, T. Mazeh and K. Innanen for helpful discussions. We also thank J. Wisdom for the use of his computers. This work was performed at the Canadian Institute for Theoretical Astrophysics and the University of Toronto, and has been supported in part by the Natural Sciences and Engineering Research Council of Canada.

#### 8. References

Benest, D., 1988, Astron. Astrophys. 206, 143.

Benest, D., 1989, Astron. Astrophys. 223, 361.

Benest, D., 1993, Cel. Mech. Dyn. Astron. 56, 45.

Benest, D., 1996, Astron. Astrophys. **314**, 983.

Black, D., 1982, Astron. J. 87, 1333.

Butler, R. P., Marcy G., Williams, E., Hauser, H. and Shirts, P., 1997, Astrophys. J. Lett. 474, L115.

Cochran, W., Hatzes, A., Butler, P. and Marcy, G., 1997, Astrophys. J 483, 457.

Dvorak, R., 1984, Cel. Mech. 34, 369.

Dvorak, R., 1986, Astron. Astrophys. 167, 379.

Dvorak, R., Froeschle, Ch., Froeschle, Cl., 1989, Astron. Astrophys. 226, 335.

Graziani, F. and Black, D., 1981, Astrophys. J. 251, 337.

Hagel, J. and Dvorak, R., 1988, Cel. Mech. 42, 355.

Hénon, M., Guyot, M., 1970, in *Periodic Orbits, Stability, and Resonances*, ed. G.E.O. Giacaglia (Dordrecht:Reidel), p. 349.

Hoffleit, D. and Jaschek, C., 1982, The Bright Star Catalogue, 4<sup>th</sup> edition, (New Haven: Yale University Observatory)

Holman, M., Touma, J. and Tremaine, S., 1997, Nature 386, 254.

Innanen, K., Zheng, J., Mikkola, S., and Valtonen, M., 1997, Astron. J 113, 1915.

Mardling, R.A. and Aarseth, S.J. 1998, NATO ASI series, in press.

Pendleton, Y. J. and Black, D.C., 1983, Astron. J. 88, 1415.

Rabl, G., Dvorak, R., 1988, Astron. Astrophys. 191, 385.

Szebehely, V., 1980, Cel. Mech. 22, 7.

Szebehely, V. and McKenzie, R., 1981, Cel. Mech. 23, 3.

Wiegert, P. A. and Holman, M. J., 1997, Astron. J. 113, 1445.

Wisdom, J. and Holman, M., 1991, Astron. J. 102, 1528.

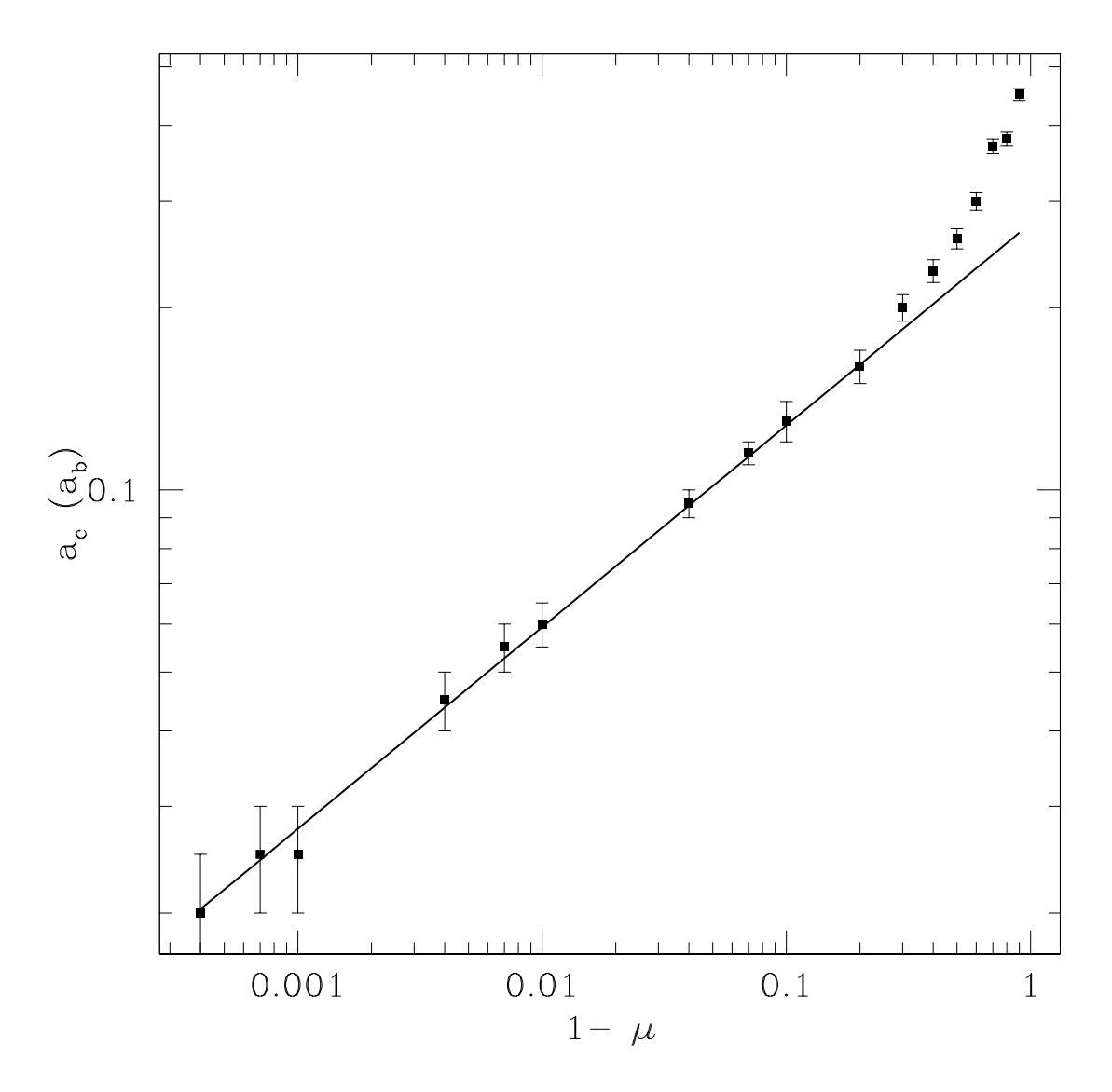


Fig. 1.— The critical semimajor axis  $a_c$  as a function of  $1 - \mu$  for the binary eccentricity e = 0. The heavy line indicates the  $(1 - \mu)^{1/3}$  dependence of the Hill's sphere. The error bars used in this and the following figures indicate the full separation between simulated particles *i.e.* if the particle separation is  $0.01a_b$ , the error bars span  $\pm 0.01a_b$ .

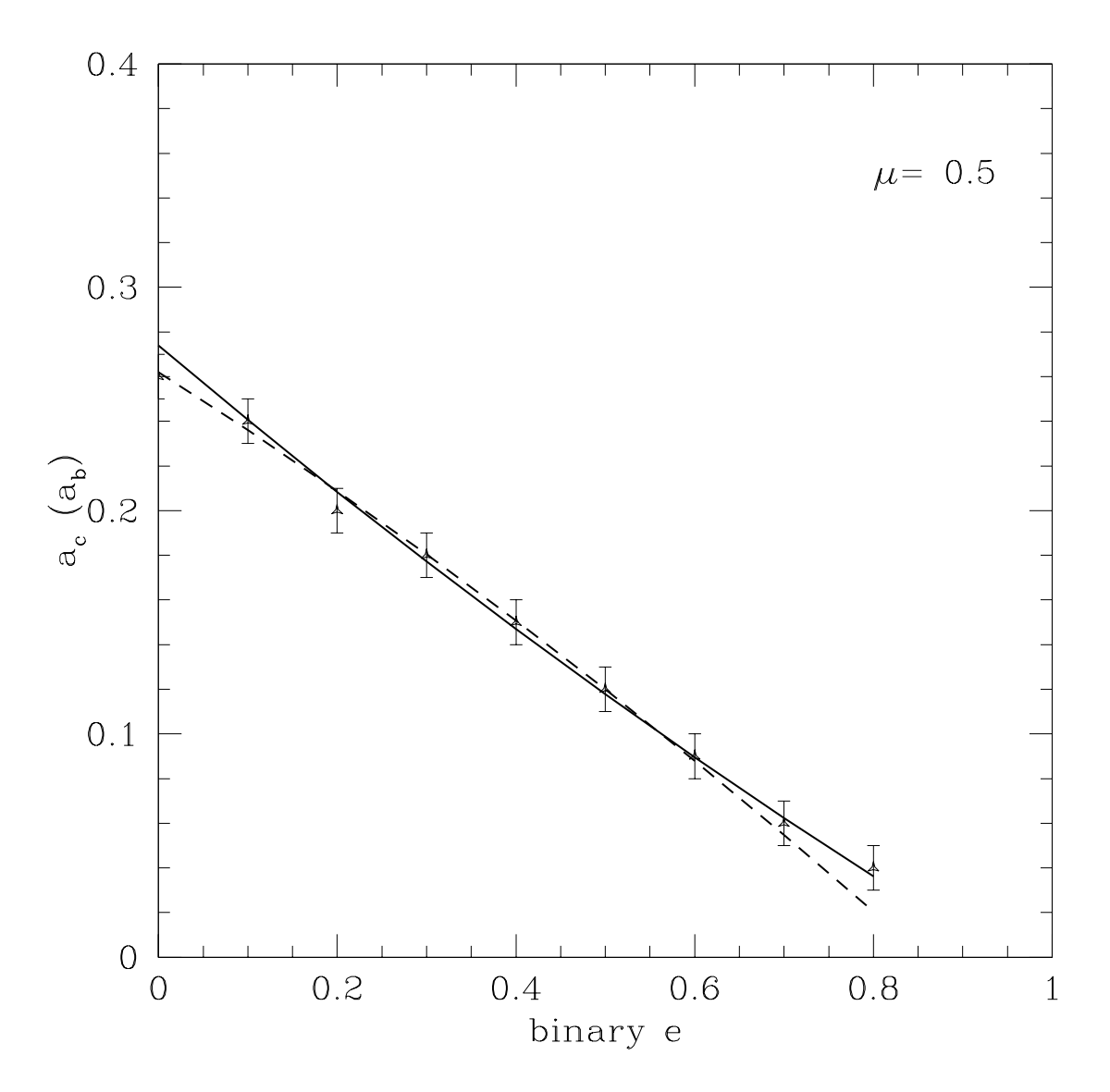


Fig. 2.— The critical semimajor axis as a function of the binary eccentricity for  $\mu=0.5$  (equal masses). The solid line is the least squares fit to results in this paper plotted for the range of eccentricity studied. The dashed line is the empirical fit reported by Rabl and Dvorak (1988). It is clear that the two are consistent.

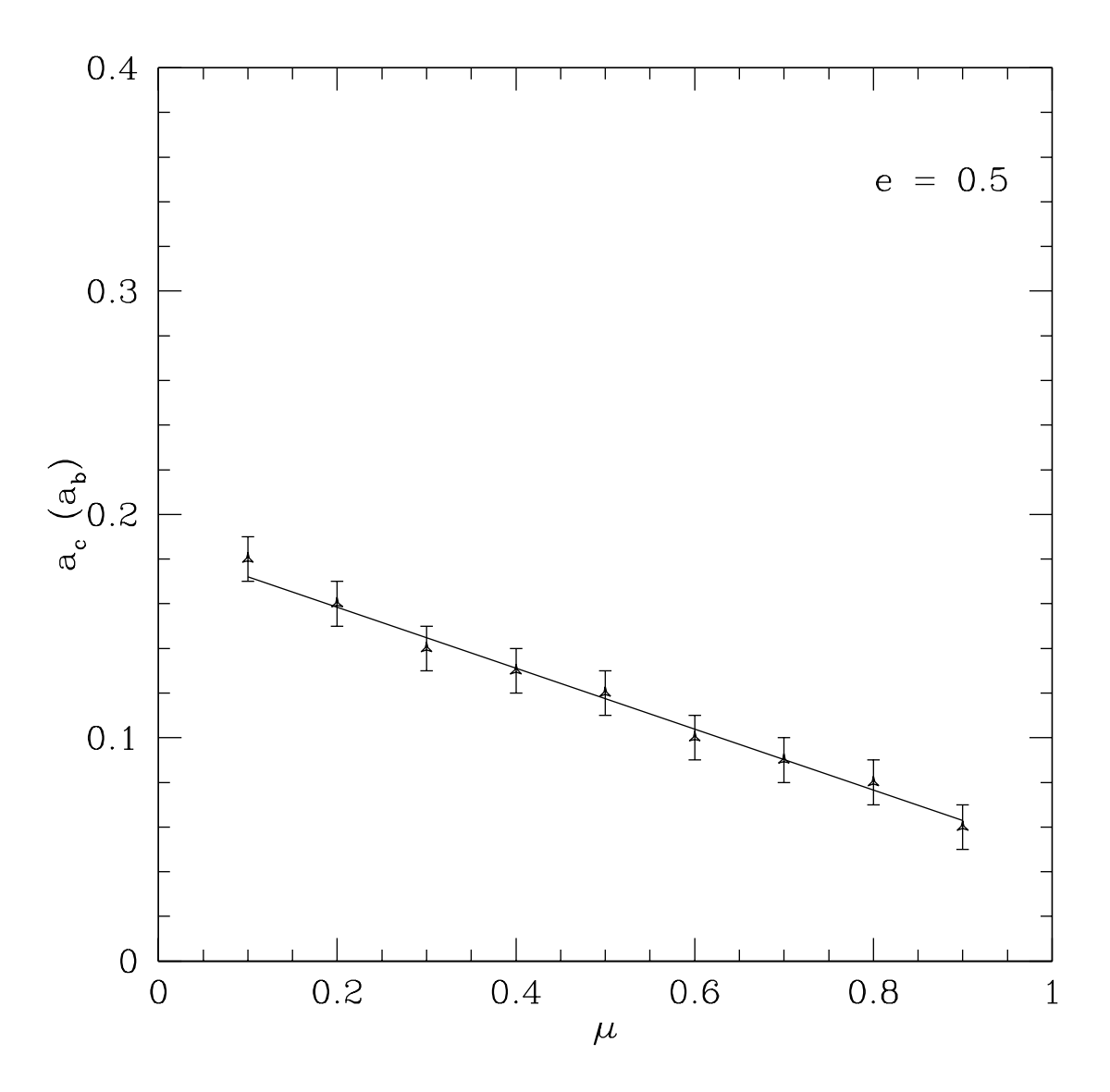


Fig. 3.— The critical semimajor axis as a function of the binary mass ratio  $\mu$  for e=0.5. The least squares fit is plotted for the range of mass ratios studied.

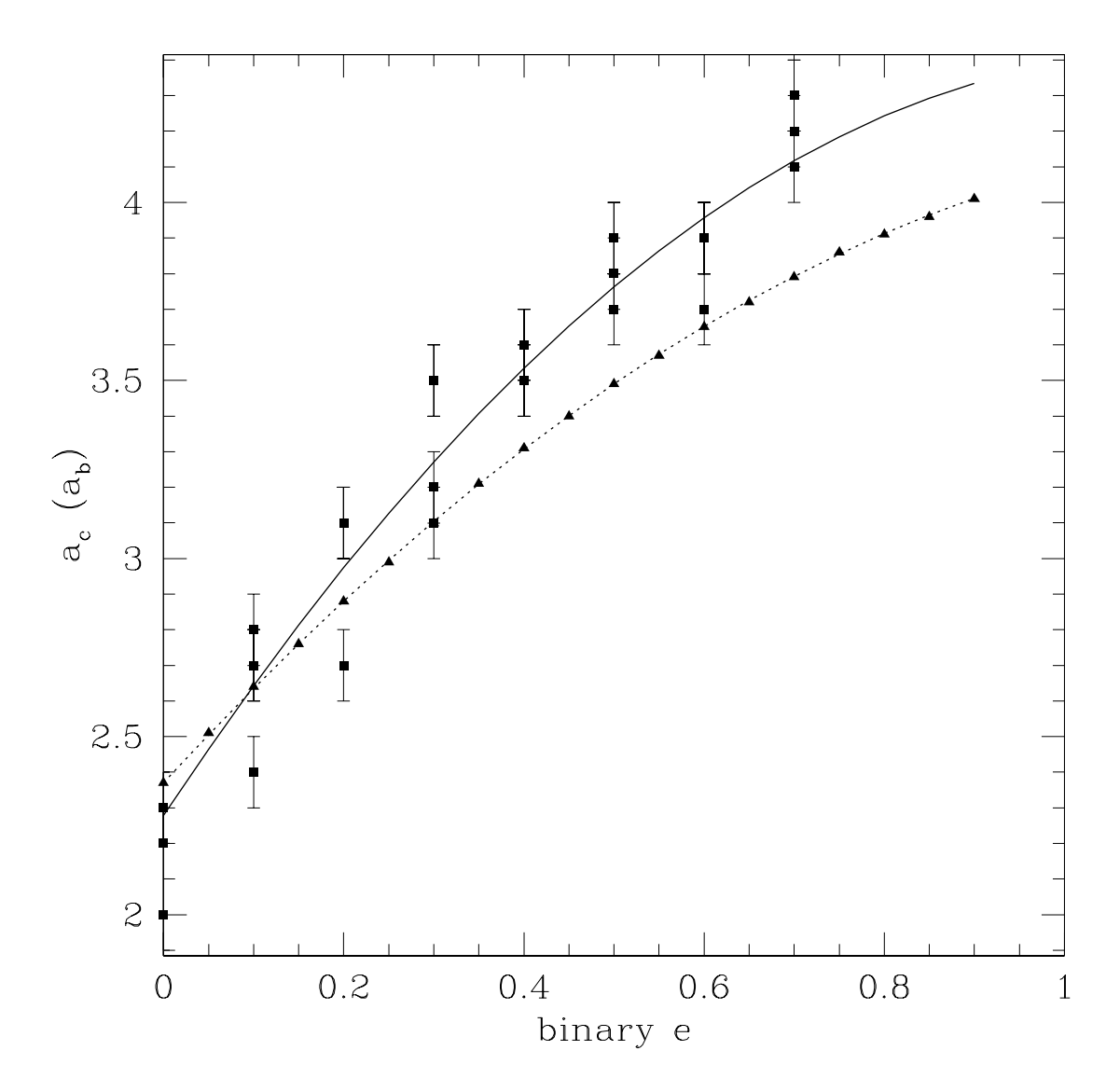


Fig. 4.— The critical semimajor axis as a function of eccentricity in the outer (P-type) region. The square data points are our results (note: four different values of  $\mu$  from 0.1 to 0.5 are used), the triangles, those of Dvorak et al. (1989). Our least-squares fit (up to quadratic in e, Eq. 5) is shown by the heavy-line, that of Dvorak et al. (see text) by a dotted line. Our simulations were run 20 times longer (10<sup>4</sup> binary periods) and indicate that there is an erosion of the stable outer region over time, at least at higher eccentricities.